

AD-A285 301



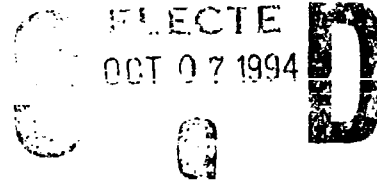
AD

TECHNICAL REPORT ARCCB-TR-94023

THE EFFECTS OF FATIGUE LOADING FREQUENCY
ON FATIGUE LIFE OF HIGH-STRENGTH
PRESSURE VESSEL STEELS

ROBERT R. FUJCAK

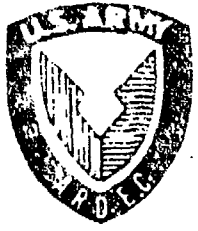
DTIC
ELECTE
OCT 07 1994



94-31838

239Y

JUNE 1994

 **US ARMY ARMAMENT RESEARCH,
DEVELOPMENT AND ENGINEERING CENTER**
CLOSE COMBAT ARMAMENTS CENTER
BENÉT LABORATORIES
WATERVLIET, N.Y. 12189-4050 

APPROVED FOR PUBLIC RELEASE; DISTRIBUTION UNLIMITED

DTIC QUALITY INSPECTED 2

9 4 1 0 0 0 3

DISCLAIMER

The findings in this report are not to be construed as an official Department of the Army position unless so designated by other authorized documents.

The use of trade name(s) and/or manufacturer(s) does not constitute an official indorsement or approval.

DESTRUCTION NOTICE

For classified documents, follow the procedures in DoD 5200.22-M, Industrial Security Manual, Section II-19 or DoD 5200.1-R, Information Security Program Regulation, Chapter IX.

For unclassified, limited documents, destroy by any method that will prevent disclosure of contents or reconstruction of the document.

For unclassified, unlimited documents, destroy when the report is no longer needed. Do not return it to the originator.

REPORT DOCUMENTATION PAGE

Form Approved
OMB No. 0704-0188

Public reporting burden for this collection of information is estimated to average 1 hour per response, including the time for reviewing instructions, searching existing data sources, gathering and maintaining the data needed, and completing and reviewing the collection of information. Send comments regarding this burden estimate or any other aspect of this collection of information, including suggestions for reducing this burden, to Washington Headquarters Services, Directorate for Information Operations and Reports, 1215 Jefferson Davis Highway, Suite 1204, Arlington, VA 22202-4302, and to the Office of Management and Budget, Paperwork Reduction Project (0704-0188), Washington, DC 20503.

1. AGENCY USE ONLY (Leave blank)	2. REPORT DATE June 1994	3. REPORT TYPE AND DATES COVERED Final
---	------------------------------------	--

4. TITLE AND SUBTITLE THE EFFECTS OF FATIGUE LOADING FREQUENCY ON FATIGUE LIFE OF HIGH-STRENGTH PRESSURE VESSEL STEELS	5. FUNDING NUMBERS AMCMS No. 6111.02.H611.1 PRON No. 1A11Z1CANMBJ
--	--

6. AUTHOR(S) Robert R. Fuczak

7. PERFORMING ORGANIZATION NAME(S) AND ADDRESS(ES) U.S. Army ARDEC Benet Laboratories, SMCAR-CCB-TL Watervliet, NY 12189-4050	8. PERFORMING ORGANIZATION REPORT NUMBER ARCCB-TR-94023
---	---

9. SPONSORING / MONITORING AGENCY NAME(S) AND ADDRESS(ES) U.S. Army ARDEC Close Combat Armaments Center Picatinny Arsenal, NJ 07806-5000	10. SPONSORING / MONITORING AGENCY REPORT NUMBER
--	---

11. SUPPLEMENTARY NOTES

12a. DISTRIBUTION / AVAILABILITY STATEMENT Approved for public release; distribution unlimited.	12b. DISTRIBUTION CODE
---	-------------------------------

13. ABSTRACT (Maximum 200 words) Bend specimens of high-strength pressure vessel steel were tested in bending fatigue to failure at 1.5, 15, 30, and 75 Hz fatigue loading frequencies. In the 1.5 to 15 Hz range, there was no discernible difference in the frequency effect on fatigue life. However, in the 30 to 75 Hz range, there was a definite increase in fatigue life compared to the lower range of frequency. The average increase in fatigue life over the stress range was a factor of 10 greater than the life at the lower frequency range. This factor increased at lower stresses and decreased at higher stresses, but even at the highest stresses tested, the increase was significant, about 5 to 1. This indicates that the frequency effect is more effective at high-cycle fatigue and diminishes with low-cycle fatigue. A model for fatigue life deterioration caused by superimposition of loads under different frequencies is introduced.
--

14. SUBJECT TERMS Fatigue Life, High Strength, Pressure Vessels, Steel, Frequency	15. NUMBER OF PAGES 17
---	----------------------------------

16. PRICE CODE

17. SECURITY CLASSIFICATION OF REPORT UNCLASSIFIED	18. SECURITY CLASSIFICATION OF THIS PAGE UNCLASSIFIED	19. SECURITY CLASSIFICATION OF ABSTRACT UNCLASSIFIED	20. LIMITATION OF ABSTRACT UL
--	---	--	---

TABLE OF CONTENTS

	<u>Page</u>
ACKNOWLEDGEMENTS	ii
INTRODUCTION	1
MATERIAL	1
SPECIMEN CONFIGURATION AND TEST MACHINES USED	1
STRESS EQUATIONS	1
TEST RESULTS AND DISCUSSION	2
FATIGUE LIFE SUPERIMPOSITION MODEL	3
CONCLUSIONS	4

TABLES

1. Bend Fatigue Data for Four Test Loading Frequencies	5
2. Combined Fatigue Life for 1.5 and 15 Hz	6
3. Combined Fatigue Life for 1.5 and 30 Hz	7
4. Combined Fatigue Life for 1.5 and 75 Hz	8

LIST OF ILLUSTRATIONS

1. Fatigue specimen schematic	9
2. Bend test loading schematic	10
3. Effects of low-frequency cyclic loading on fatigue life of ASTM A723 steel	11
4. Effects of high-frequency cyclic loading on fatigue life of ASTM A723 steel	12
5. Effects of fatigue loading frequency rate on fatigue life of ASTM A723 steel	13
6. Fatigue life deterioration for 15 Hz superimposed on 1.5 Hz	14
7. Fatigue life deterioration for three rates superimposed on 1.5 Hz	15

ACKNOWLEDGEMENTS

I wish to thank Joseph Kapp for his technical guidance, Ronald Abbott of the Materials Science Branch for his technical assistance in the many phases of the test program, Daniel Corrigan of the Experimental Mechanics Branch for his drafting assistance, and Ellen Fogarty and Rose Neifeld of the Technical Publications and Editing Office for their editing assistance.

Accession For	
NTIS CRA&I	<input checked="" type="checkbox"/>
DTIC TAB	<input type="checkbox"/>
Unannounced	<input type="checkbox"/>
Justification	
By	
Distribution	
Availability	
Dist	Avail and/or Special
A-1	

INTRODUCTION

High frequency, high amplitude dynamic strain waves are produced in high-strength pressure vessels during cyclic loading. Consideration must be given to the effect of these strain waves on fatigue life, since the pressure vessel is subjected to more than one strain cycle per operation cycle.

MATERIAL

The high-strength material used in this program is A723 steel with a 0.2 percent offset yield strength of 966 MPa (140 Ksi) and an ultimate tensile strength of 1035 MPa (150 Ksi).

SPECIMEN CONFIGURATION AND TEST MACHINES USED

Figure 1 shows a schematic diagram of the bending test specimen designed for the range of loading frequencies tested: 1.5, 15, 30, and 75 Hz. Figure 2 shows a schematic of the loading configuration on the bend specimens. An Instron Model 1350 fatigue testing machine with a 45 kN (10,000-pound) capacity was used for the tests at 1.5 and 15 Hz. For 30 Hz, a Sonntag fatigue testing machine was used because of its fixed frequency of operation. For the final frequency, 75 Hz, an Instron Model 1603 electromagnetic resonance machine capable of 50 to 400 Hz was used.

We attempted to achieve 150 Hz with this specimen configuration, but the Instron Model 1603 machine only allowed a peak of 75 Hz for this size specimen. In order to reach 150 Hz, a smaller specimen is needed, so we were unable to test beyond 75 Hz with the available systems and the specific specimen design.

STRESS EQUATIONS

The maximum stress, S , on the outside surface in bending is represented by the following well-known bending equation:

$$S = Mc/I \quad (1)$$

where $M =$ bending moment $= Pl/2 \quad (2)$

$P =$ bending load

$l =$ moment arm length

$c =$ distance from center to outer surface $= b/2 \quad (3)$

$b =$ cross-sectional vertical specimen height

$I =$ moment of inertia $= Bb^3/12 \quad (4)$

$B =$ cross-sectional horizontal specimen width

The substitution of equations (2), (3), and (4) into equation (1) yields the following equation:

$$S = 3Pl/(Bb^2) \quad (5)$$

Since this equation is calculated for reverse bending where the stress ratio, R , between S_{max} and S_{min} is $R = -1$, the loads had to be recalculated for this test program, because we used a stress ratio of $R = 0$, or $S_{min} = 0$. To give a root mean square comparison for $R = 0$, the maximum loads were multiplied by 1.414 for the one-sided loading program.

TEST RESULTS AND DISCUSSION

The bend specimens were tested to failure in groups at the four different frequencies in order to generate fatigue data curves. Table 1 represents the bending fatigue test results using $R = 0$ at the four loading frequencies tested.

Figure 3 shows a comparison of the effects of two low frequencies, 1.5 and 15 Hz, on bending fatigue life of A723 steel. Examination of both sets of data indicates there may be a slight improvement in fatigue life with increase in loading rate from 1.5 to 15 Hz, but statistically it is very small. Note that the individual scatter is greater than the difference between both sets. This indicates that there is not enough difference within this range to be considered significant.

Consider the next range of loading frequency data represented in Figure 4. In this case, there is a slightly larger difference between the effects from 30 to 75 Hz than the difference noted between 1.5 and 15 Hz, but even in this case the difference is not very large. The 75 Hz loading rate contributes an average increase of about 50 percent compared to 30 Hz.

The greatest surprise comes from examination of Figure 5, which displays the spectrum of results. Figure 5 shows that the improvement in fatigue life contributed by the 30 Hz loading rate compared to 15 Hz is the greatest even though the frequency ratio is only doubled. All the other ratios are greater than 2-to-1, but do not enhance the fatigue life accordingly with equivalent loading frequency rate. For instance, the response in fatigue life improvement gained by the increase of loading rate from 15 Hz to 30 Hz (2-to-1) shows an average increase of 8-to-1, whereas the improvement gained from 1.5 Hz to 75 Hz (50-to-1) shows an average increase in life of 15-to-1. Therefore, the greatest improvement within this limited range occurred between 15 and 30 Hz loading rate, suggesting some type of step phenomenon in the intermediate frequency range.

Upon examination of the slopes of the regression curves in Figure 5, it is apparent that the effects of fatigue life improvement by increase in loading frequency rate become minimized at very high stresses, as shown by the convergence of the lines at the upper left portion of the graph. This indicates that fatigue life improvement is a high-cycle phenomenon and contributes very little in the low-cycle fatigue range. The greatest improvements can be experienced at stresses with fatigue cycle failures from 10,000 cycles and on, especially at higher cycles and lower stresses, because the fanning effect contributes increasing payoffs in fatigue life improvement as the curves diverge at lower stresses.

Conversely, if high-frequency waves are superimposed upon conditions under high stress and in or near the low-cycle fatigue range, these added cycles caused by possible strain waves may be disastrous in taking away remaining fatigue life from the original cyclic source. As the operating stress is lowered, these additional high-frequency cycles diminish their effect, so it is important to find a suitable operating range that will effectively wash out this effect.

FATIGUE LIFE SUPERIMPOSITION MODEL

Reflecting back to Figure 3, we can determine that there is little, if any, difference in fatigue life caused by a loading rate of 1.5 or 15 Hz. Indeed, a least squares analysis indicates that the correlation coefficient, r , for both sets of data is 0.939, demonstrating a good logarithmic straight-line fit. In this case, superimposition of an equal load at 15 Hz upon an applied load at 1.5 Hz costs ten cycles added on to each cycle at 1.5 Hz, or the equivalent damage of eleven cycles, producing an equivalent fatigue life of 1/11th of the single loading. Figure 6 shows this effect applied to superimposition of 15 Hz on 1.5 Hz. The deterioration factor may be worse for stresses at or near 1000 MPa approaching yield values, and may diminish for stresses lower than 400 MPa, where the endurance limit may be reached.

The following model describes fatigue life deterioration as applied to the fatigue data presented in this report. When the superimposed frequency, Hz_s , is greater than the applied loading rate, Hz_a , then the cyclic loss factor is defined as

$$CLF = Hz_s/Hz_a \quad (6)$$

The mitigation factor, MF, is defined as the ratio between fatigue life of the superimposed loading rate by itself, N_s , and the fatigue life of the applied loading rate, N_a , or

$$MF = N_s/N_a \quad (7)$$

The mitigation factor then becomes a way of "mitigating" the effects of a cyclic loading rate that allows more cycles-to-failure by itself than the applied rate.

Thus, the effective cyclic loss factor, CLF_e , is defined as

$$CLF_e = CLF/MF \quad (8)$$

In the case of 15 Hz superimposed upon 1.5 Hz, the mitigation factor washes out to become 1, and has no mitigating effect on the effective fatigue life in superimposition. That explains why the effective life curve is constantly at 1/11th of the applied life curve alone. Table 2 displays fatigue life values for 1.5 and 15 Hz and the deterioration of the fatigue life by combining the two frequencies in superimposition. In this case, superimposition of a 15 Hz wave over an applied 1.5 Hz causes the fatigue life to deteriorate to 1/11th of the fatigue life with the applied 1.5 Hz load alone.

Additionally, this fatigue life model was used for superimposition of 30 Hz and 75 Hz on the applied 1.5 Hz, with the results displayed in Figure 7. In these examples, the mitigation factor starts low at high stresses and increases as stresses decrease. This is indicated by the differences in the slopes between the 1.5 Hz line and the 30 Hz and 75 Hz lines.

Table 3 displays the calculated deterioration of fatigue life by combining the fatigue lives at 1.5 Hz and 30 Hz in superimposition. Table 4 displays a similar deterioration in fatigue life by combining 1.5 Hz and 75 Hz. Both Tables 3 and 4 indicate that the deterioration effect caused by superimposition diminishes as the applied stress drops.

CONCLUSIONS

1. Under a high-stress, low-cycle fatigue environment, high-frequency dynamic strains are detrimental to the fatigue life because they rob cycles from the remaining life by superimposition, and cause the structure to fail prematurely.

2. Since remaining fatigue life increases with an increase in loading frequency as the operating stress is lowered, the detrimental effect can be minimized or nullified by designing an operating stress low enough to enable high-cycle fatigue life.

3. The minimization of the effects of high-frequency strains occurs at low operating stresses because the fanning-away effect of the slope changes in the high cycle range. It becomes more and more forgiving as the operating stress is lowered.

4. The model indicates that the frequency effect may be detrimental when superimposed upon a lower frequency at a high operating stress, but may disappear entirely at lower stresses, again suggesting an operating stress design criterion at reasonably low stresses.

Table 1. Bend Fatigue Data for Four Test Loading Frequencies

Loading Frequency (Hz)	Stress Ksi (MPa)	Cycles to Failure
1.5	150 (1035)	15,131
	140 (966)	18,908
	120 (808)	45,246
	115 (793)	44,007
	110 (759)	172,928
	100 (690)	112,285
15	150 (1035)	18,500
	140 (966)	25,700
	120 (828)	56,500
	115 (793)	80,000
	115 (793)	61,000
	110 (759)	146,200
	100 (690)	156,100
	95 (655)	200,400
30	150 (1035)	58,000
	130 (897)	363,000
75	170 (1173)	32,000
	160 (1104)	68,000
	150 (1035)	74,000
	140 (966)	210,000
	130 (897)	599,000
	120 (828)	1,300,000

Table 2. Combined Fatigue Life for 1.5 and 15 Hz

Stress (MPa)	N (1.5)	N (15)	N Ratio	Combined N
1,381	2,118	2,118	0.0909	193
1,300	3,111	3,111	0.0909	283
1,200	5,176	5,176	0.0909	471
1,100	9,002	9,002	0.0909	818
1,000	16,505	16,505	0.0909	1,500
900	32,259	32,259	0.0909	2,933
800	68,231	68,231	0.0909	6,203
700	159,522	159,522	0.0909	14,502
600	425,218	425,218	0.0909	38,656
500	1,355,864	1,355,864	0.0909	123,261
400	5,605,030	5,605,030	0.0909	509,550
300	34,930,637	34,930,637	0.0909	3,175,526
200	460,439,513	460,439,513	0.0909	41,858,299

Table 3. Combined Fatigue Life for 1.5 and 30 Hz

Stress (MPa)	N (1.5)	N (30)	N Ratio	Combined N
1,381	2,118	1,440	0.0329	70
1,300	3,111	3,125	0.0478	149
1,200	5,176	8,717	0.0777	402
1,100	9,002	26,587	0.1287	1,158
1,000	16,505	90,190	0.2146	3,542
900	32,259	347,998	0.3504	11,303
800	68,231	1,574,481	0.5357	36,552
700	159,522	8,716,688	0.7321	116,779
600	425,218	62,853,449	0.8808	374,541
500	1,355,864	650,281,255	0.9600	1,301,587
400	5,605,030	11,352,249,745	0.9902	5,550,223
300	34,930,637	453,182,933,827	0.9985	34,876,872
200	460,439,513	81,851,448,561,775	0.9999	460,387,716

Table 4. Combined Fatigue Life for 1.5 and 75 Hz

Stress (MPa)	N (1.5)	N (75)	N Ratio	Combined N
1,381	2,118	4,540	0.0411	87
1,300	3,111	8,851	0.0538	167
1,200	5,176	21,427	0.0765	396
1,100	9,002	56,021	0.1107	996
1,000	16,505	160,529	0.1628	2,688
900	32,259	514,001	0.2417	7,796
800	68,231	1,827,839	0.3562	24,306
700	159,522	8,211,066	0.5085	81,113
600	425,218	45,286,124	0.6805	289,367
500	1,355,864	339,277,356	0.8335	1,130,059
400	5,605,030	3,989,938,361	0.9344	5,237,173
300	34,930,637	95,711,997,923	0.9821	34,304,653
200	460,439,513	8,432,714,870,322	0.9973	459,185,899

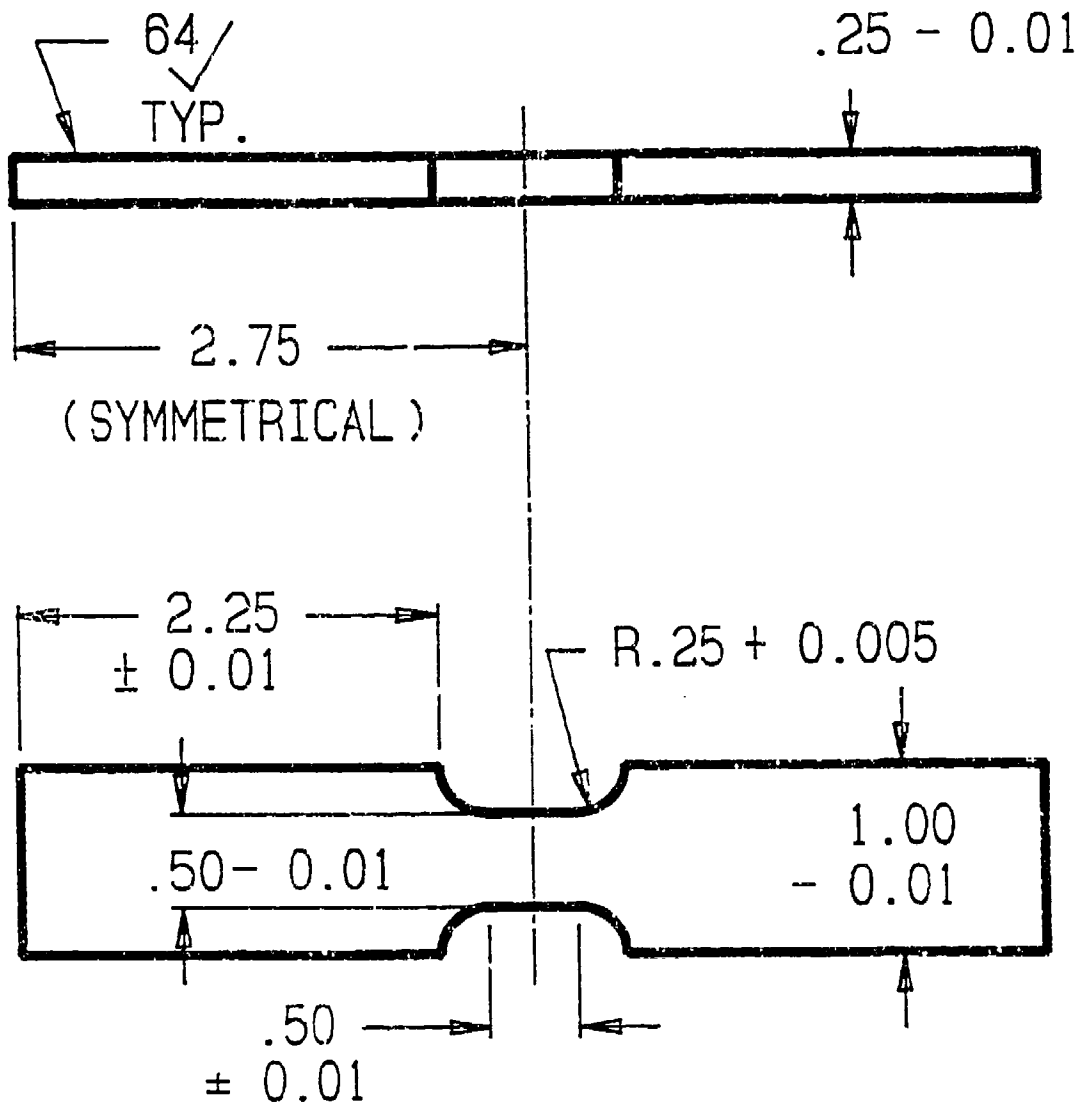


Figure 1. Fatigue specimen schematic.

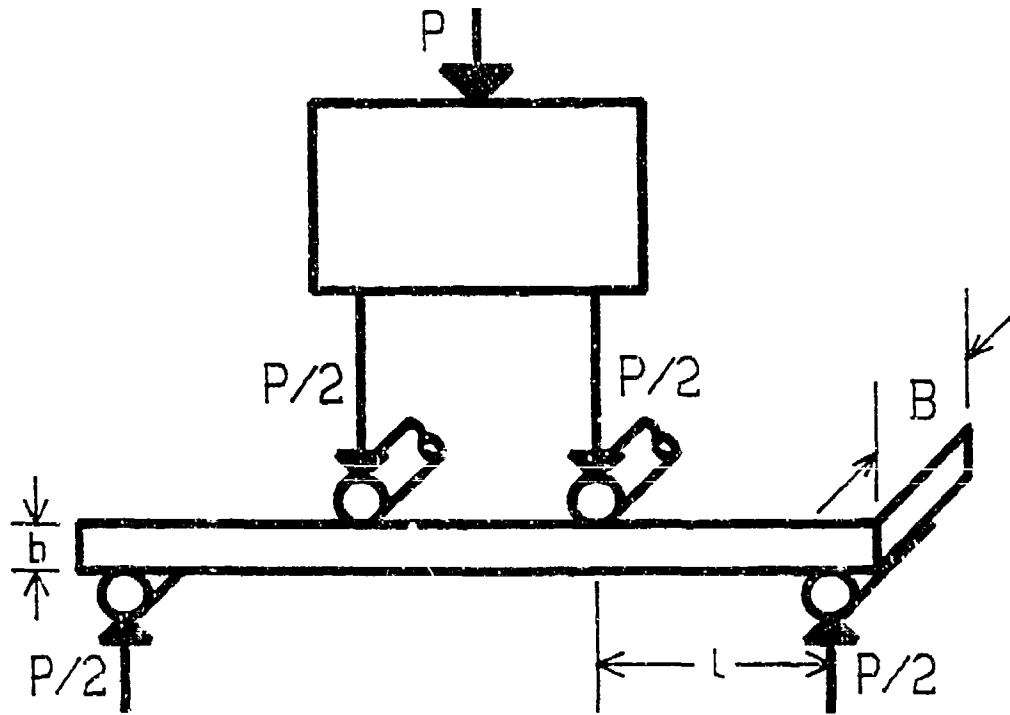
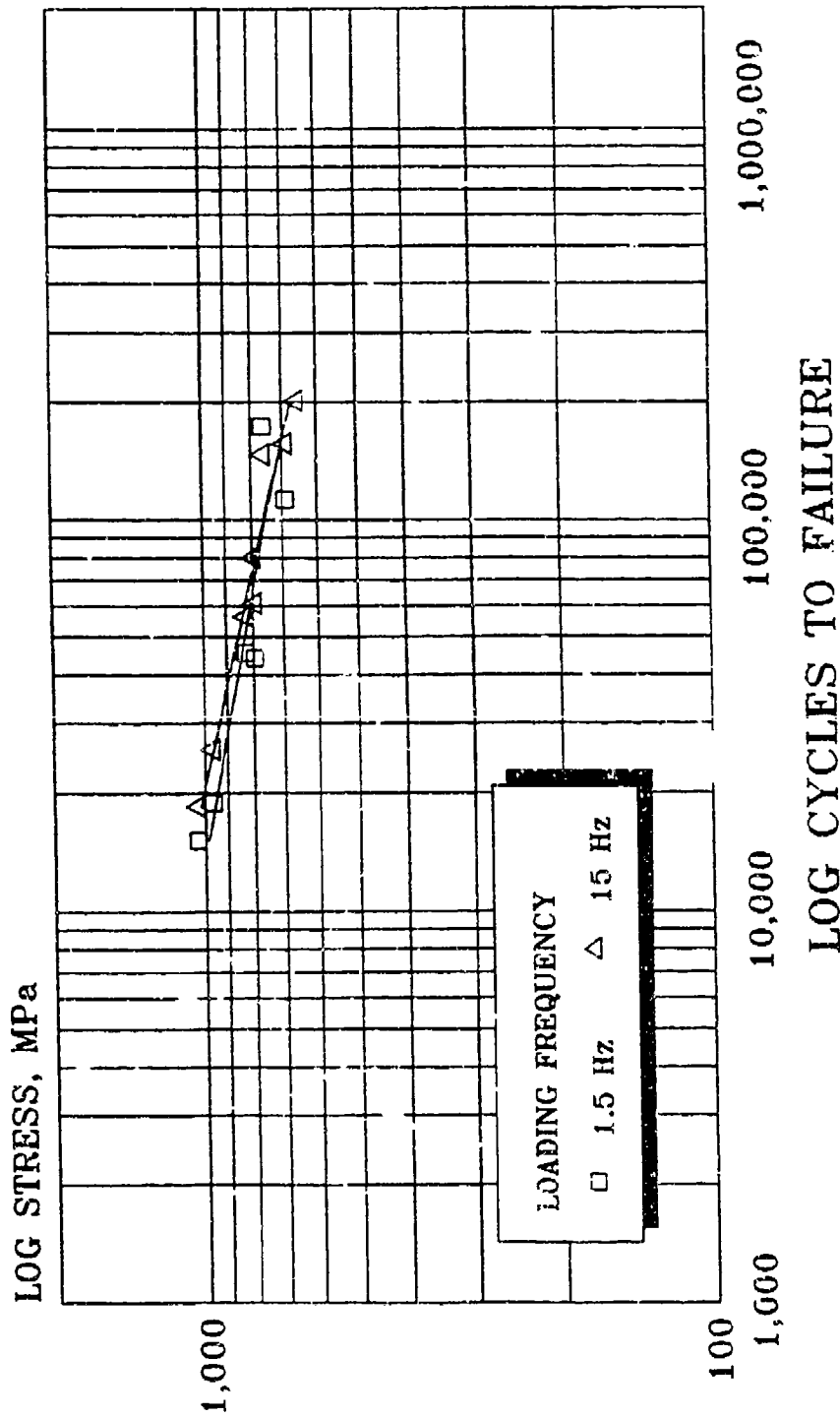


Figure 2. Bend test loading schematic.

BENDING FATIGUE CHART

STRESS vs. CYCLES TO FAILURE

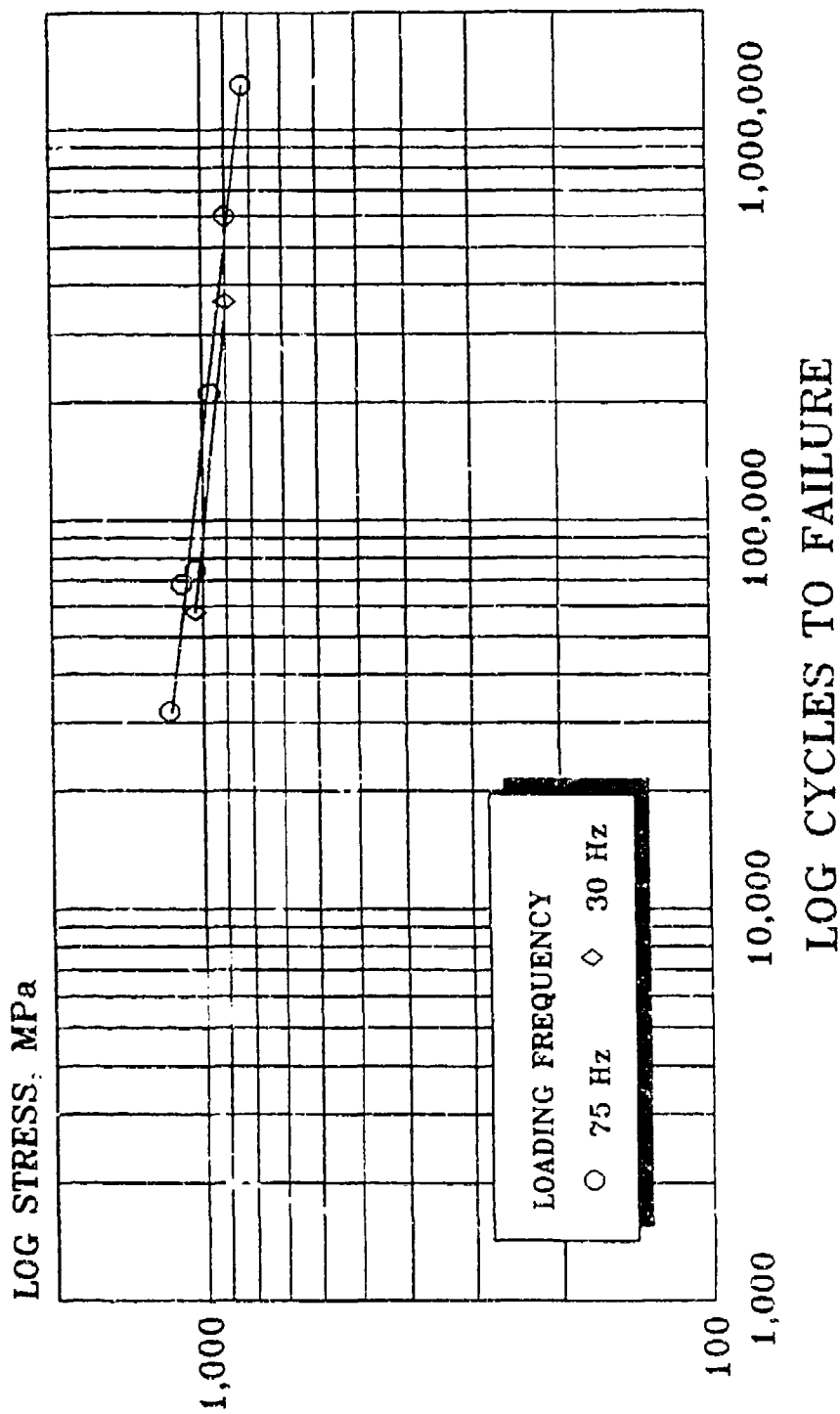


FOR 1.5 AND 15 Hz LOADING RATE
 ASTM A723 BEND SPECIMENS, R = 0

Figure 3. Effects of low-frequency cyclic loading on fatigue life of ASTM A723 steel.

BENDING FATIGUE CHART

STRESS vs. CYCLES TO FAILURE

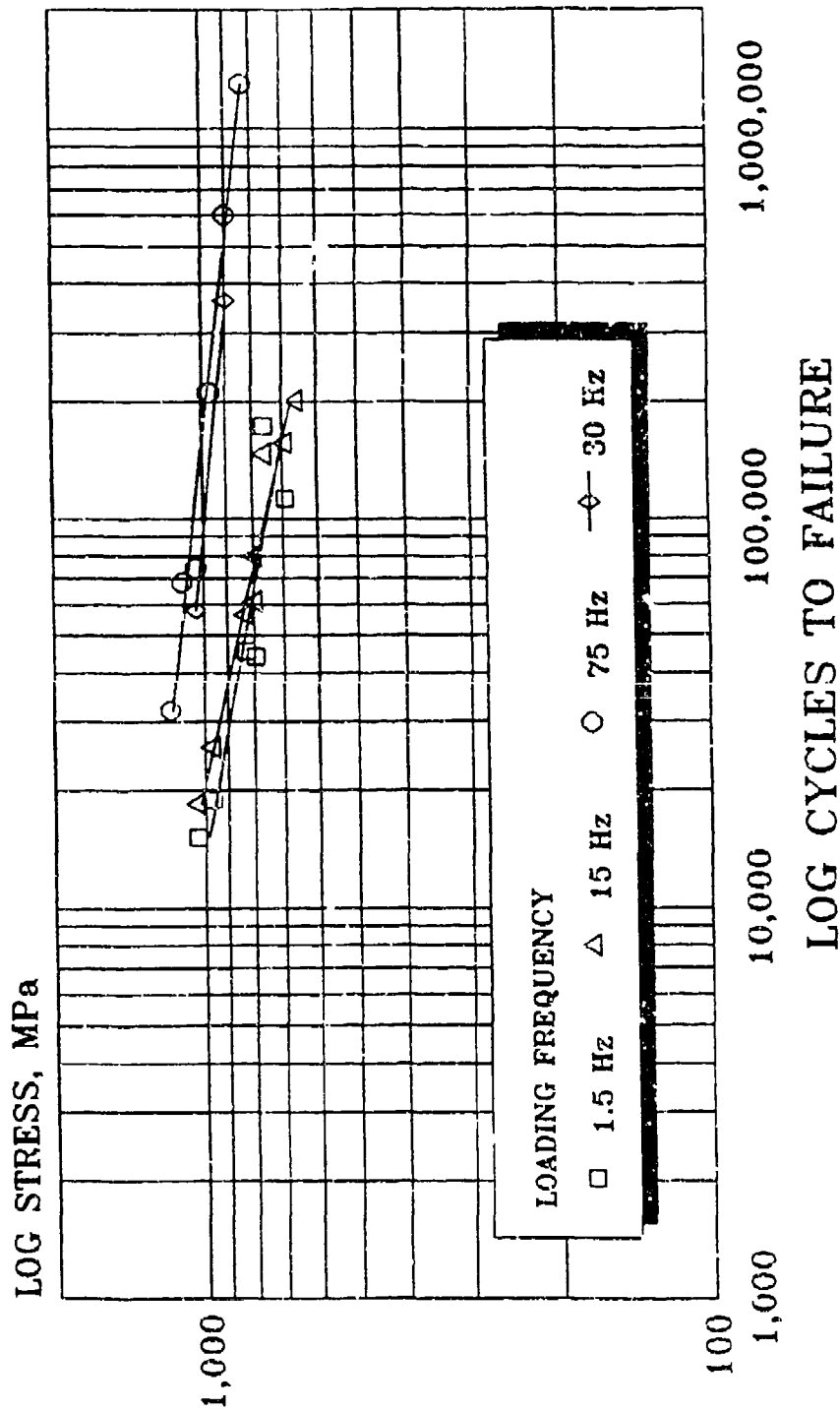


FOR 30 AND 75 Hz LOADING RATES
 ASTM A723 BEND SPECIMENS, R = 0

Figure 4. Effects of high-frequency cyclic loading on fatigue life of ASTM A 723 steel.

BENDING FATIGUE CHART

STRESS vs. CYCLES TO FAILURE



FOR 1.5, 15, 30 AND 75Hz LOADING RATES
 ASTM A723 BEND SPECIMENS, R = 0

Figure 5. Effects of fatigue loading frequency rate on fatigue life of ASTM A723 steel.

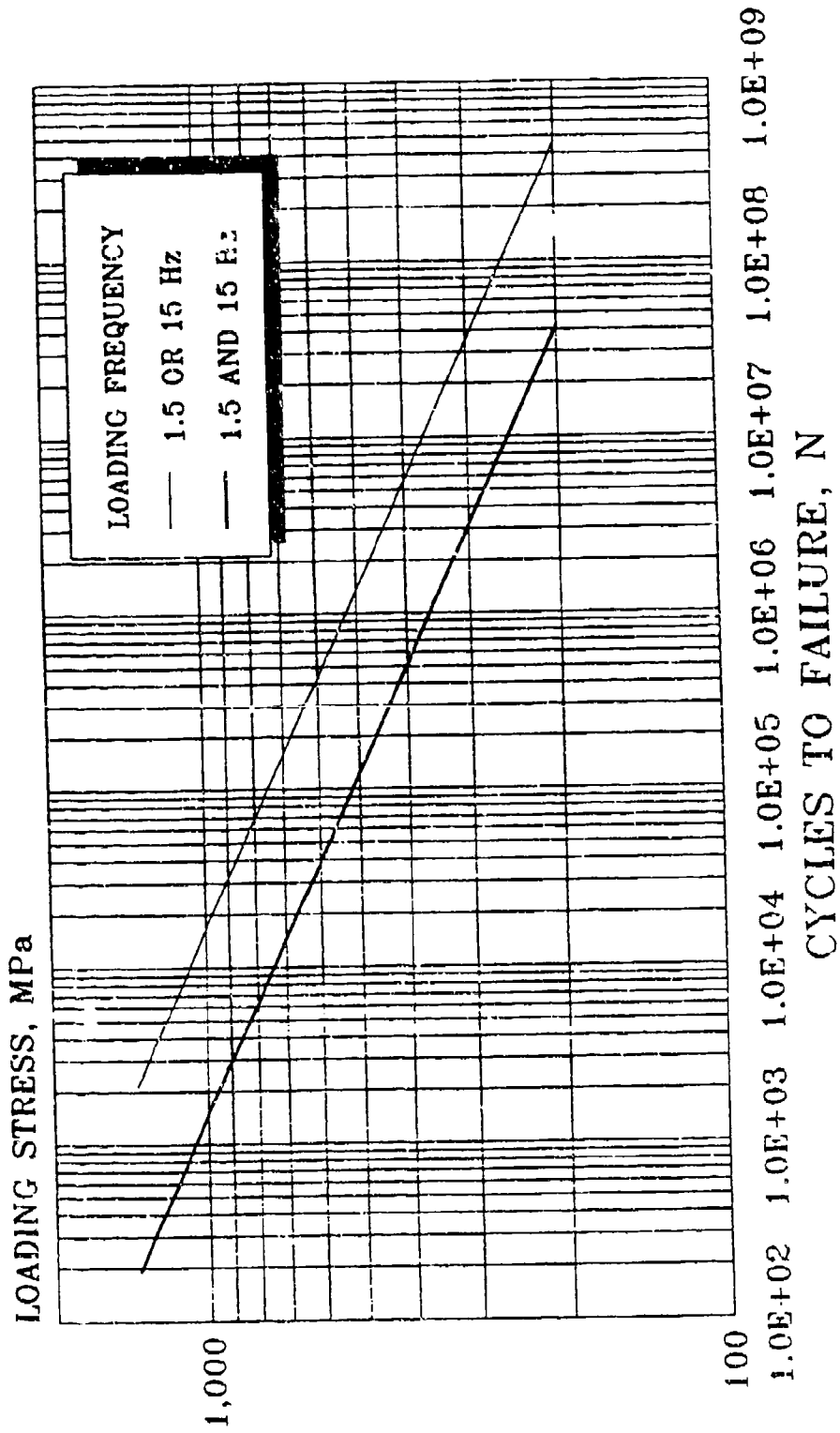


Figure 6. Fatigue life deterioration for 15 Hz superimposed on 1.5 Hz.

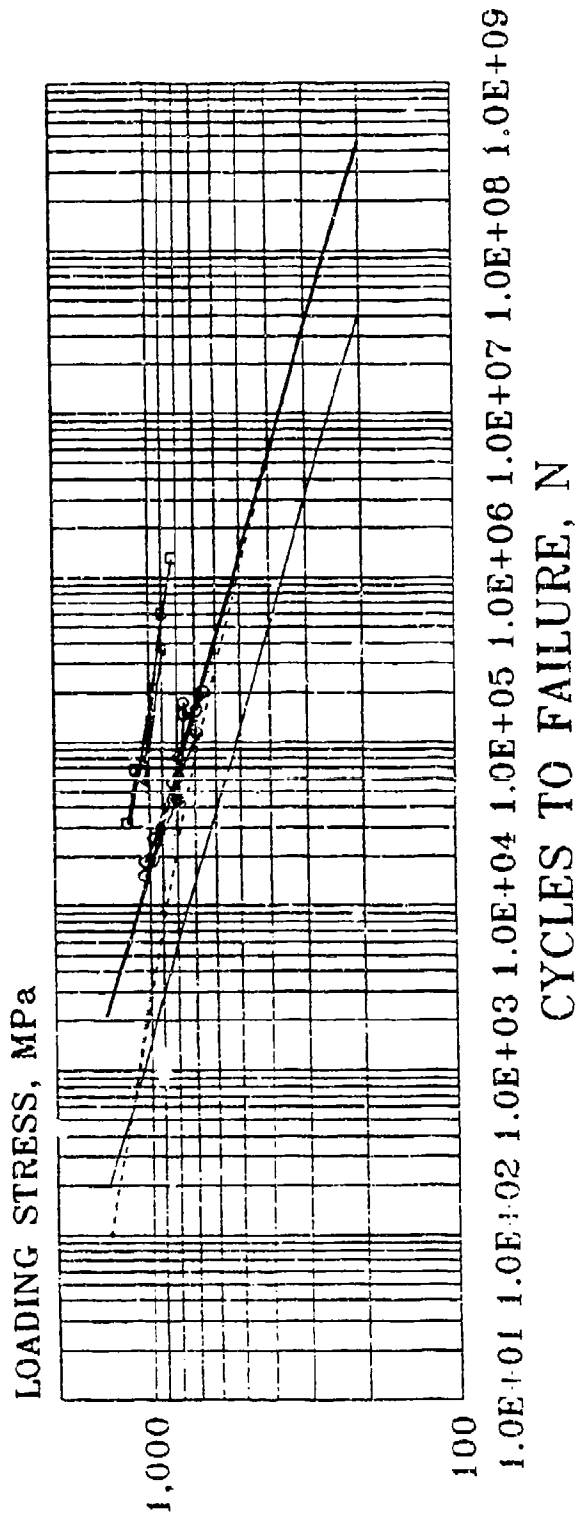
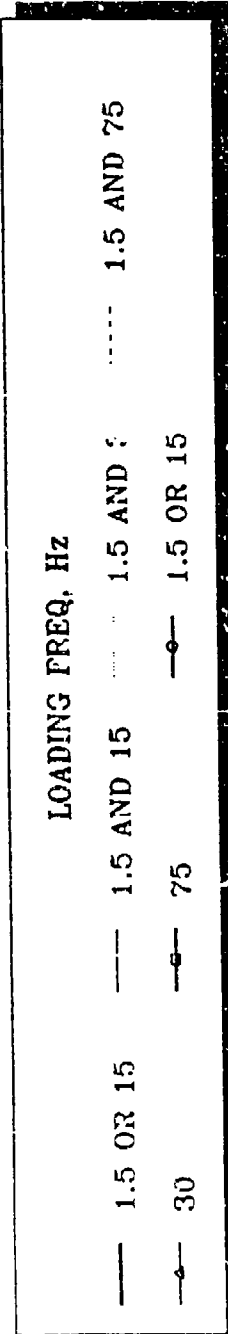


Figure 7. Fatigue life deterioration for three rates superimposed on 1.5 Hz.

TECHNICAL REPORT INTERNAL DISTRIBUTION LIST

	<u>NO. OF COPIES</u>
CHIEF, DEVELOPMENT ENGINEERING DIVISION	
ATTN: SMCAR-CCB-DA	1
-DC	1
-DI	1
-DR	1
-DS (SYSTEMS)	1
CHIEF, ENGINEERING DIVISION	
ATTN: SMCAR-CCB-S	1
-SD	1
-SE	1
CHIEF, RESEARCH DIVISION	
ATTN: SMCAR-CCB-R	2
-RA	1
-RE	1
-RM	1
-RP	1
-RT	1
TECHNICAL LIBRARY	
ATTN: SMCAR-CCB-TL	5
TECHNICAL PUBLICATIONS & EDITING SECTION	
ATTN: SMCAR-CCB-TL	3
OPERATIONS DIRECTORATE	
ATTN: SMCWV-ODP-P	1
DIRECTOR, PROCUREMENT & CONTRACTING DIRECTORATE	
ATTN: SMCWV-PP	1
DIRECTOR, PRODUCT ASSURANCE & TEST DIRECTORATE	
ATTN: SMCWV-QA	1

NOTE: PLEASE NOTIFY DIRECTOR, BENÉT LABORATORIES, ATTN: SMCAR-CCB-TL OF ADDRESS CHANGES.

TECHNICAL REPORT EXTERNAL DISTRIBUTION LIST

	<u>NO. OF COPIES</u>		<u>NO. OF COPIES</u>
ASST SEC OF THE ARMY RESEARCH AND DEVELOPMENT ATTN: DEPT FOR SCI AND TECH THE PENTAGON WASHINGTON, D.C. 20310-0103	1	COMMANDER ROCK ISLAND ARSENAL ATTN: SMCRI-ENM ROCK ISLAND, IL 61299-5000	1
ADMINISTRATOR DEFENSE TECHNICAL INFO CENTER ATTN: DTIC-FDAC CAMERON STATION ALEXANDRIA, VA 22304-6145	12	MIAC/CINDAS PURDUE UNIVERSITY P.O. BOX 2634 WEST LAFAYETTE, IN 47906	1
COMMANDER U.S. ARMY ARDEC ATTN: SMCAR-AEE	1	COMMANDER U.S. ARMY TANK-AUTMV R&D COMMAND ATTN: AMSTA-DDL (TECH LIBRARY) WARREN, MI 48397-5000	1
SMCAR-AES, BLDG. 321	1	COMMANDER U.S. MILITARY ACADEMY ATTN: DEPARTMENT OF MECHANICS WEST POINT, NY 10966-1792	1
SMCAR-AET-O, BLDG. 351N	1		
SMCAR-FSA	1		
SMCAR-FSM-E	1		
SMCAR-FSS-D, BLDG. 94	1		
SMCAR-IMI-I, (STINFO) BLDG. 59	2	U.S. ARMY MISSILE COMMAND REDSTONE SCIENTIFIC INFO CENTER ATTN: DOCUMENTS SECTION, BLDG. 4484 REDSTONE ARSENAL, AL 35898-5241	2
PICATINNY ARSENAL, NJ 07806-5000			
DIRECTOR U.S. ARMY RESEARCH LABORATORY ATTN: AMSRL DD-T, BLDG. 305 ABERDEEN PROVING GROUND, MD 21005-5066	1	COMMANDER U.S. ARMY FOREIGN SCI & TECH CENTER ATTN: DRXST-SD 220 7TH STREET, N.E. CHARLOTTESVILLE, VA 22901	1
DIRECTOR U.S. ARMY RESEARCH LABORATORY ATTN: AMSRL-WT-PD (DR. B. BURNS) ABERDEEN PROVING GROUND, MD 21005-5066	1	COMMANDER U.S. ARMY LABCOM MATERIALS TECHNOLOGY LABORATORY ATTN: SLCMT-IML (TECH LIBRARY) WATERTOWN, MA 02172-0001	2
DIRECTOR U.S. MATERIEL SYSTEMS ANALYSIS ACTV ATTN: AMXSY-MP ABERDEEN PROVING GROUND, MD 21005-5071	1	COMMANDER U.S. ARMY LABCOM, ISA ATTN: SLCIS-IM-TL 2800 POWER MILL ROAD ADELPHI, MD 20783-1145	1

NOTE: PLEASE NOTIFY COMMANDER, ARMAMENT RESEARCH, DEVELOPMENT, AND ENGINEERING CENTER, U.S. ARMY AMCCOM, ATTN: BENET LABORATORIES, SMCAR-CCB-TL, WATERVLIET, NY 12189-4050 OF ADDRESS CHANGES.

TECHNICAL REPORT EXTERNAL DISTRIBUTION LIST (CONT'D)

	<u>NO. OF COPIES</u>		<u>NO. OF COPIES</u>
COMMANDER U.S. ARMY RESEARCH OFFICE ATTN: CHIEF, IPO P.O. BOX 12211 RESEARCH TRIANGLE PARK, NC 27709-2211	1	COMMANDER AIR FORCE ARMAMENT LABORATORY ATTN: AFATL/MN EGLIN AFB, FL 32542-5434	1
DIRECTOR U.S. NAVAL RESEARCH LABORATORY ATTN: MATERIALS SCI & TECH DIV CODE 26-27 (DOC LIBRARY) WASHINGTON, D.C. 20375	1	COMMANDER AIR FORCE ARMAMENT LABORATORY ATTN: AFATL/MNF EGLIN AFB, FL 32542-5434	1

NOTE: PLEASE NOTIFY COMMANDER, ARMAMENT RESEARCH, DEVELOPMENT, AND ENGINEERING CENTER, U.S. ARMY AMCCOM, ATTN: BENÉT LABORATORIES, SMCAR-CCB-TL, WATERVLIET, NY 12189-4050 OF ADDRESS CHANGES.
